Journal of Computer-Aided Molecular Design, **15:** 13–27, 2001.
KLUWER/ESCOM

Screening the molecular surface of human anticoagulant protein C: A search for interaction sites

Bruno O. Villoutreix[a,*], David G. Covell[b], Anna M. Blom[c], Anders Wallqvist[b,d], Ute Friedrich[c] & Björn Dahlbäck[c]

[a]*School of Pharmacy, INSERM U428, 4 Ave. de l'Observatoire, F-75006 Paris, France;* [b]*Frederick Cancer Research and Development Center, National Cancer Institute, Science Applications International Corporation, Frederick, MD 21702, U.S.A.;* [c]*Lund University, The Wallenberg Laboratory, Dept. of Clinical Chemistry, University Hospital, Malmö, S-205 02 Malmö, Sweden;* [d]*Rutgers University, Department of Chemistry, P.O. Box 939, Piscataway, NJ 08855-0939, U.S.A.*

Received 5 January 2000; Accepted 13 June 2000

Key words: coagulation, protein C, protein interaction, protein modelling, thrombin

Summary

Protein C (PC), a 62 kDa multi-modular zymogen, is activated to an anticoagulant serine protease (activated PC or APC) by thrombin bound to thrombomodulin on the surface of endothelial cells. PC/APC interacts with many proteins and the characterisation of these interactions is not trivial. However, molecular modelling methods help to study these complex biological processes and provide basis for rational experimental design and interpretation of the results. PC/APC consists of a Gla domain followed by two EGF modules and a serine protease domain. In this report, we present two structural models for full-length APC and two equivalent models for full-length PC, based on the X-ray structures of Gla-domainless APC and of known serine protease zymogens. The overall elongated shape of the models is further cross-validated using size exclusion chromatography which allows evaluation of the Stokes radius (r_s for PC = 33.15 Å; r_s for APC = 34.19 Å), frictional ratio and axial ratio. We then propose potential binding sites at the surface of PC/APC using surface hydrophobicity as a determinant of the preferred sites of intermolecular recognition. Most of the predicted binding sites are consistent with previously reported experimental data, while some clusters highlight new regions that should be involved in protein-protein interactions.

Abbreviations: PC, protein C; APC, activated protein C; T, thrombin; TM, thrombomodulin; Gla-domain, γ-carboxyglutamic-rich domain; EGF, epidermal growth factor; FVa, activated factor V; FVIIIa, activated factor VIII; FVIIa, activated factor VII; FIXa, activated factor IX; EPCR, endothelial protein C/APC receptor; SP, serine protease; r_s, Stokes radius; 1 Å = 0.1 nm; f/f_0, frictional ratio; a/b, axial ratio. The chymotrypsinogen nomenclature for APC/thrombin is used throughout the text while the protein C numbering is indicated between parentheses if appropriate. P3, P2, P1 and P1′, P2′, P3′ . . . designate inhibitor residues amino- and carboxy-terminal to the scissile peptide bond, respectively, and S1, S2 . . . and S1′, S2′ . . . the corresponding subsites on the active protease side.

Introduction

The protein C (PC) anticoagulant pathway is a vital system which appears to be more complex than originally envisioned [reviewed in 1–3]. Protein C (a zymogen) is activated by thrombin (T) bound to thrombomodulin (TM), a transmembrane protein expressed on the surface of endothelial cells. The essential role of activated protein C (APC), a trypsin-like serine protease, is downregulation of the coagulation cascade through limited degradation of two membrane-bound cofactors, factor Va (FVa) and factor VIIIa (FVIIIa)

*To whom correspondence should be addressed. E-mail: villoutreix@pharmacie.univ-paris5.fr

[reviewed in 4]. For the time being, these are the only known substrates for APC, while the reasons for this specificity are not yet fully understood. Degradation of FVa and FVIIIa is enhanced by the presence of a non-enzymatic cofactor, protein S (PS), and the inactivation of FVIIIa seems to also be potentiated by a second cofactor, factor V (FV) [5, 6]. APC is inhibited by molecules from the serpin family: protein C inhibitor (PCI) and α1-antitrypsin and by the 'macromolecular cage', α2-macroglobulin. Residues in APC involved in interactions with its cofactors, substrates or inhibitors are not known in detail. Similarly, the amino acids in contact with the thrombin-thrombomodulin (T-TM) complex during the activation process are still not well defined.

PC (419 residues) is produced mostly in the liver as a single-chain inactive zymogen which is proteolytically processed before secretion (removal of K156 and R157) to a two-chain molecule [7]. Under physiological conditions, APC is generated after a specific proteolytic cleavage within the activation peptide of PC (between R169 and L170, P1 residue: R169) by thrombin (T), preferentially when the latter is bound to TM. Binding of thrombin to soluble TM results in a drastic (2000-fold) enhancement of the PC activation rate, while a similar reaction in the presence of membrane-bound TM increases the activation rate by about 20 000-fold [8]. Upon activation by the T-TM complex, the 12 amino acid activation peptide of PC is released (residues 158 to 169) [8, 9]. Different molecular mechanisms have been proposed to explain the role of TM during the activation process but several points remain unclear [9, 10]. A recently identified molecule named endothelial protein C/APC receptor (EPCR) appears to enhance the activation of PC by the T-TM complex [reviewed in 1]. Possibly, EPCR binds to the Gla-domain of PC/APC.

From a structural standpoint, PC is a multidomain vitamin K-dependent plasma glycoprotein that has the same modular organisation as many other blood coagulation enzymes (e.g., factor VII (FVII) or factor IX (FIX)). Protein C consists of a phospholipid binding γ-carboxyglutamic acid (Gla)-rich domain (which binds at least 7 calcium ions), two epidermal growth factor (EGF)-like domains and a serine protease domain. The Gla-EGF1-EGF2 region constitutes the light chain while the serine protease (SP) domain is referred to as the heavy chain. These two chains are covalently linked via a disulphide bond which bridges C141 in the light chain to C122 (residue 277 in the PC numbering) in the heavy chain. The 3D structure of human Gla-domainless APC has been solved by X-ray crystallography [11] but a full-length APC model would be valuable. Since the 3D structure of Gla domains is well conserved and because the X-ray structures of full-length human FVIIa in complex with tissue factor and of porcine FIXa are known [12–14], it is possible to develop a reasonable model of full-length APC. Furthermore, fluorescence energy transfer studies or X-ray/neutron scattering have shown that the active sites of FVIIa, APC and FIXa are situated at about 82 Å, 94 Å and 80 Å, from the membrane plane, respectively, and that FVIIa adopts a fully extended conformation also in solution [15–18]. However, despite the fact that these multi-modular blood coagulation enzymes appear to all have an extended rod-like structure, different spatial organisation within the light chain region can be observed. Indeed, when comparing the structures of FIXa, FVIIa and Gla-domainless APC, the SP and EGF2 domains are organized in a similar fashion and the angle between the Gla and EGF1 domains of FVIIa and of FIXa can be considered as similar. Differences between these three proteins are noted at the EGF1-EGF2 intermodule angle. Therefore, it is possible to propose several models for APC/PC with differences at the level of the EGF1-EGF2 interface.

Availability of a three-dimensional (3D) structure is of major importance to help designing experiments. In fact, structural data enable molecular biologists to focus site directed mutagenesis, thereby saving time and effort as compared to the standard random approach. In the present post-genomic era, a tremendous amount of information can be found in sequence and structural databases and one goal of bioinformatics is to rationalize and exploit these data. Because 3D folds have evolved at a much slower rate than amino acid sequences, it is possible to predict the structure (e.g., a Gla-domain) of a protein by homology modelling or related methods. The exact angle between two modules is however difficult to foresee, but approximate conformations can be proposed and in most cases they are sufficient to gain insights into molecular mechanisms. Many research projects aim initially at the identification of binding sites at the surface of proteins and computer analysis of molecules can also provide significant insights. Forces that attract proteins towards each other have been divided, for the sake of simplification, into hydrophobic and electrostatic [19–27]. Clusters of solvent exposed hydrophobic or charged amino acids tend to signal hot spots on the molecules and it is thus possible to pro-

pose recognition sites, using theoretical means [19, 28–30].

In the present report, we attempted to probe the structure-function relationships of APC/PC using molecular modelling methods. A first step along this line was to develop models for full-length APC that would be consistent with the overall dimensions of the molecule as deduced from fluorescence energy transfer experiments [16] and X-ray crystallography studies of Gla-domainless APC [11]. The next step was to derive equivalent models for the zymogen form using the two full-length APC-models as initial framework, while taking into account information from related zymogen structures [31, 32]. In parallel, the hydrodynamic properties of APC/PC were analyzed, using size exclusion chromatography, which allows for calculations of Stokes radius, frictional and axial ratios, and estimation of the overall shape of the molecules. Although the method used here to predict binding sites has been applied to many systems [19, 28–30] we decided to test again this approach on the X-ray structure of thrombin [33], since key residues involved in the interaction between thrombin and TM have been recently fully identified via X-ray crystallography [34]. The molecular surfaces of the APC/PC-models were then screened and residues, possibly forming recognition sites, were defined.

Materials and methods

The X-ray structure of the calcium loaded bovine prothrombin (Gla-domain and kringle 1) (2.2 Å resolution, entry 2pf2) [35] was obtained from the Protein Data Bank (PDB) [36] and selected as a template to build the Gla module of protein C. The method (sequence alignment, energy minimization and structural analysis) to build the Gla-domain of protein C has been reported before [12, 37]. The other experimental structures used here were Gla-domainless human APC (2.8 Å resolution, entry 1aut) [11], factor IXa (3.0 Å resolution, entry 1pfx) [14] and FVIIa coordinates extracted from the FVIIa-tissue factor complex (2 Å resolution, entry 1dan) [13]. The X-ray structure of thrombin [33], as modified in Reference 10, has been described earlier. The X-ray structures of chymotrypsinogen (1.8 Å resolution, entry 2cga) [31] and prethrombin 2 (2 Å resolution, entry 1hag) [32] were used to build models for PC.

Modelling full-length APC/PC molecules

Two models were built for full-length APC. In the first model (model 1), the predicted Gla domain of APC was grafted onto the Gla-domainless X-ray structure, using the same angle as observed in the structure of FVIIa. This approach is acceptable, as this segment in both proteins has the same length. In the second model (model 2), the EGF1 and Gla domain of APC were both relocated in space to follow the orientation observed in FVIIa. Amino acid side chains of the APC-model were then re-oriented, if necessary, using low-energy rotamer conformations [38]. The connecting regions between the Gla-domain and the EGF1 or between the EGF1 and EGF2 were built interactively and refined via short rounds of energy minimisation, using the simulation program Discover (Biosym-MSI, San Diego, CA, USA), in order to optimise the geometry of these segments and to remove possible steric overlaps. Because there are eight residues between the last Cys residue of the PC EGF1-domain (C89) and the first Cys of the second EGF (C98) and nine residues in the equivalent region of FVII, we assumed that the more extended conformation of the FVII light chain could serve as an approximate template for protein C modelling (see Figure 1).

The X-ray structure of the serine protease domain of APC was used as a starting conformation to generate a model for the zymogen form as reported in Reference 10, while including information from chymotrypsinogen and prethrombin 2 structures [31, 32]. The size and sequence similarity between prethrombin 2 and PC activation peptide regions suggest however that prethrombin 2 should be selected to guide the prediction of this region of protein C (Figure 1). There are 27 residues between PC C141 and R169 (the peptide bond cleaved by thrombin during PC activation is the one between R169 and L170, residue 16 in the chymotrypsinogen numbering), while prethrombin 2 has 26 residues in the equivalent position. Chymotrypsinogen has only 13 residues there, clearly indicating that this structure is less appropriate as initial template, while still of interest during the modelling process. Thus, homology modelling based upon the structure of prethrombin 2 and a loop search protocol were used to build an initial model for the activation peptide segment of PC. This region (backbone angles) was not forced to fit into the active site of a serine protease and should approximately represent the activation peptide of protein C in a solution. A 10-ps molecular dynamics simulation at 10 K was then performed on the SP

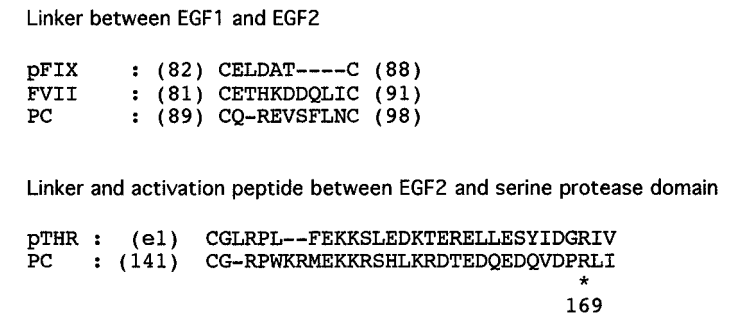

Figure 1. Sequence of linker and activation peptide regions of PC and related molecules. The * indicates the Arg-residue, after which the peptide bond is cleaved during activation (residue 169 in PC). The numbering for pTHR follows the one used in the PDB-file. PC refers to the human PC/APC sequence; pTHR, to human prethrombin 2; hFVII, to human factor VII and pFIX to porcine factor IX.

domain of PC, in order to smoothly readjust the structure after the departure of residue 170 region from its buried location in the activated conformation form of the SP domain and to slightly modify the S1 specificity pocket and oxyanion hole areas. These calculations took into account the second EGF domain which was however restrained to its original conformation as observed in the X-ray structure of Gla-domainless APC. This approach is appropriate because the EGF2 is on the other side of the molecule as compared to the activation peptide area. Then, the modelled serine protease zymogen domain was grafted onto the two light chain models built above in order to generate PC model 1 and PC model 2.

Proteins

Human and bovine PC were expressed in human kidney cell line 293 (ATCC no. 1573-CRL) and purified by anion exchange chromatography with calcium-elution [39]. PC was activated by thrombin as described previously and both proteins (PC, APC) were characterized functionally as described in Reference 39.

Gross conformation of APC/PC in solution

The proteins were applied to a Superose 12 gel (Amersham Pharmacia), equilibrated with Tris-HCl; pH 7.6, 150 mM NaCl (TBS), supplemented with 2.5 mM $CaCl_2$ or 5 mM EDTA. About 600 μl of the protein solution (25 μg) was applied at a flow of 0.5 ml/min and the absorbance of the eluate was continuously measured at 280 nm. The calibration curve was obtained as previously [40, 41], using as protein standards: thyroglobulin (r_s = 85 Å; Mw = 669 kDa), ferritin (r_s = 61 Å; Mw = 440 kDa), catalase (r_s = 52.2 Å; Mw = 232 kDa), aldolase (r_s = 48.1 Å; Mw = 158 kDa), bovine serum albumin (r_s = 35.5 Å; Mw = 65 kDa), ovalbumin (r_s = 30.5 Å; Mw = 43 kDa), chymotrypsinogen A (r_s = 20.9 Å; Mw = 25 kDa) and ribonuclease A (r_s = 16.4 Å; Mw = 13.7 kDa), which were all obtained from Amersham Pharmacia. Gel filtration data were expressed in terms of Kav, being a distribution coefficient which is defined as: Kav = (Ve − Vo) / (Vt − Vo); where Ve is the elution volume of the protein, Vo is the void volume of the column determined using blue dextrane (Amersham Pharmacia) and Vt is the total volume of the column evaluated with thymidine (Sigma). There is a relationship between the elution volume expressed in terms of Kav and the Stokes radius of a protein. The $(-\log \mathrm{Kav})^{1/2}$ for standard proteins was plotted versus the corresponding Stokes radius and the radius of human APC and PC was calculated. Frictional ratios for APC and PC were evaluated, using the following equation [42]:

$$f/f_0 = r_s/(3\nu M_r/4\pi N)^{1/3},$$

where N is Avogadro's number (6.022×10^{23} mol^{-1}), ν is the partial specific volume of the protein, r_s is the Stokes radius and M_r is the molecular mass (62 000 for human PC/APC). Partial specific volumes for human APC and PC were calculated from the amino acid composition to be equal to 0.736 and 0.735 cm^3 g^{-1}, respectively. The frictional ratio is related to two molecular parameters describing the molecule in solution: shape and the molecular expansion of the molecule in solution, because of tight association with solvent molecules. The shape contribution is represented by the Perrin function (P) and the molecular expansion through solvent association is represented by the 'apparent hydration' (δ), which is the mass of aqueous solvent, chemically or physically associated with the

molecule per unit dry mass of protein and is included in the equation:

$$P = (f/f_0)(\delta/\nu\rho_0 + 1)^{-1/3},$$

where ρ_0 is the density of water at 20 °C (0.9982 g $\times$ ml^{-1}). We then calculated the axial ratio (a/b) of the hydrodynamically equivalent prolate ellipsoid of revolution for a typical value of $\delta = 0.35\ g_{water}/g_{protein}$ based on the shape function P. The ratio a/b was obtained as described previously [43] by a numerical inversion of the equation:

$$P = [(1 - b^2/a^2)^{1/2}]/(b/a)^{2/3}$$
$$\ln[(1 + (1 - b^2/a^2)^{1/2})/(b/a)].$$

Theoretical enumeration of binding sites

A method for identification of potential binding sites has been described previously [19] but a brief summary will be presented here. A simplified model, consisting of only the Cα coordinates, was used to represent the geometry of each residue. The lattice model of Cα atoms for the protein studied here fit the molecule coordinates within 1 Å RMS deviation. Lattice positions exterior to the molecular surface can be examined for their interactions with residues of the target molecule (e.g., PC model 1 or PC model 2). This method can be considered as similar to calculating molecular surfaces based on their accessibility to a water molecule probe. The probable binding strength of each exterior position is determined by simply counting the number and type of target Cα positions within 7.5 Å of any exterior point. The amino acid composition of the defined clusters thus scores the relative strength for which a ligand might bind at that site. The binding strength for each exterior position is the sum of scores for its constituent residues: $\phi_{cluster} = \sum_{i=1}^{N} e_i$, where N is the number of neighbouring ($d < 7.5$ Å) residues. Parameters for each residue type were based on assigning a hydrophobic value, determined from residue-based contact energies as calculated by Miyazawa and Jernigan [44]. We tested our approach on the X-ray structure of thrombin [33], as modified in Reference 10. We then ran calculations on our full-length APC and PC model structures. All clusters were then analyzed interactively on the computer screen and matched, when possible, with available experimental data.

Results and discussion

The spatial relationships of the different modules of APC or PC and the way APC/PC can interact with the membrane or with other molecules (e.g., FVa, FVIIIa, serpins, protein S, EPCR) are not known in detail. Similarly, the activation process of PC by the T-TM complex is not clearly understood. However, insights into these intermolecular interactions are of considerable interest as potential targets for therapeutic regulation of blood clotting. Experimental studies of some of these complexes at the surface of phospholipid membrane via X-ray crystallography have not yet been successful, in part due to the instability of these macromolecular assemblies and/or flexibility of some protein segments. Consequently, current progress in understanding of the structure/function of these macromolecular complexes relies on the ability to combine bioinformatics with experimental data pertaining to the structure.

Full-length activated protein C models (model 1 and model 2)

We have built the holo form of the Gla-domain of PC/APC, using the calcium-loaded coordinates of prothrombin as an initial structural framework [35]. As there are no striking amino acid substitutions within the central core of the Gla domain of APC/PC when compared with prothrombin, it is clear that this region of PC adopts the same fold as the one of other Gla-domains. Indeed, the few amino acid changes within the Gla-domains of PC when compared to prothrombin, are essentially solvent exposed and thus can be easily accommodated. Thus as the 3D structure of the Gla-domain was straightforward to predict, we then focussed our attention on the remaining domains of the APC/PC models.

When comparing the X-ray structures of FVIIa and FIXa or Gla-domainless APC, some differences are observed at the level of the light chain (e.g., the intermodule angle differs). One possible way to select a candidate template to build full-length APC, is to consider the number of residues forming the connecting segment between the modules of the light chain. There are 9 residues within the linker region between the EGF1 and EGF2 (last Cys of the EGF1 and first Cys of the EGF2) in human FVII, 8 in human APC and 5 in porcine/human IX (Figure 1). The linker between the Gla-domain and the first EGF has the same length in APC and FVIIa and the Gla-EGF1 intermodule angle

can be considered similar when comparing FVIIa and FIXa. However, the location of the EGF1 in the Gla-domainless APC X-ray structure differs from the one of FVIIa. Collectively, these observations suggest that two models for APC could be developed (Figure 2). In the first model, the APC Gla-domain homology model was grafted directly onto the APC Gla-domainless X-ray structure (model 1). In the second model, the PC Gla-domain and EGF1 were relocated according to the FVIIa structure (model 2).

Several lines of evidence support the hypothesis that, in general, vitamin K-dependent blood coagulation enzymes have extended conformations. For instance, factor VIIa has a Stokes radius of 28 Å (Mw = 49 kDa) and frictional ratio of 1.39, indicating that the molecule is elongated [45], as further confirmed by X-ray crystallography [13]. We have used size-exclusion chromatography to determine the Stokes radius of human APC under different experimental conditions (with or without calcium ions). The Superose 12 column was calibrated with several proteins for which the Stokes radius is known. Subsequently, the calibration curve was used to estimate the Stokes radius of APC. The protein elutes as a single sharp peak, corresponding to a Stokes radius of 34.19 Å in the presence of calcium ions and 34.93 Å in the absence of metal ions (Table 1). The frictional ratio (f/f_0) and axial ratio (a/b) were calculated by modelling APC as a hydrodynamically equivalent prolate ellipsoid for a 'typical' value of δ ($\delta = 0.35\ g_{water}/g_{protein}$). As shown in Table 1, the frictional ratio of APC calculated from the obtained Stokes radius in the presence of calcium ions was equal to 1.302 (f/f_0 for a sphere = 1). Because the frictional ratio depends both on shape and hydration, the overall asymmetry of APC molecules is better assessed by the axial ratio a/b (3.45 for APC while a/b for a sphere = 1). The X-ray structures of blood coagulation enzymes as well as fluorescence energy transfer experiments suggest that these proteins could be modelled as prolate ellipsoids. A prolate ellipsoid is a rodlike shape with a long semiaxis 'a' and two shorter semiaxes, 'b', that are of identical length. It is known that the hydrated volume of a protein (Vh) can be approximated as $Vh = [M_r /N] (\nu + \delta\nu 1)$, where ν is the partial specific volume of the anhydrous molecule, δ, the hydration (about 0.35 $g_{water}/g_{protein}$), and $\nu 1$ the partial specific volume of pure water (about 1 cm^3/g). For APC, Vh is about 11×10^4 $Å^3$. Furthermore, the volume of a prolate ellipsoid is equal to $(4/3)\ (\pi)\ (a)b^2$. Since the axial ratio a/b for APC is equal to 3.45 (thus a = 3.45b), $Vh = (4/3)\ (\pi)\ (3.45)\ b^3$ and the semiaxes are then b = 20 Å and a = 70 Å. Thus, the total long axis for APC is predicted to be about 140 Å and the two shorter axes would be about 40 Å. The long axis of APC model 2, as measured on the computer screen, is about 130 Å (about 120 Å for APC model 1) and the molecule could fit approximately into a box, for which the two shorter b axes would be about 50 Å.

Collectively, the above results strongly suggest deviation from spherical shape and that full-length APC has an elongated conformation in solution. Comparison of data obtained in the presence and absence of calcium (Table 1) indicates that APC is slightly more extended in the absence of calcium, which most likely reflects the fact that the Gla-domain is not fully folded in the absence of metal ions and, possibly, that some modifications occur at the Gla-EGF1 interface. Similar analysis was performed for bovine APC and the results obtained were similar with the ones calculated for the human enzyme. Bovine and human APC molecules (or PC, see below) were also modelled as oblate ellipsoids and the data suggested that the proteins were elongated. In fact, the overall dimensions were about the same for these two limiting shapes which is due to the fact that the frictional properties of oblate and prolate ellipsoids become indistinguishable when the axial ratios range from about 2 to 6. However, as mentioned above, because the overall shape of Gla-domainless APC is known from X-ray crystallography, our aim here was essentially to rule out the possibility that APC (or PC) could have its Gla-domain folding back against the serine protease domain. Our results indeed support the notion that APC (PC) does not behave like a sphere in solution and has a long molecular axis of about 140 Å.

In addition to the above calculated axial ratios in solution and overall dimensions of the Gla-domainless APC molecule as determined by X-ray crystallography, previously reported fluorescence energy transfer measurements suggest also that full-length APC has an elongated shape. These measurements can be taken into account during the modelling process, further guiding the development of realistic 3D models. Thus, the overall size of APC should match a distance of about 94 Å observed between the membrane surface and the active site region [16]. Assuming that the membrane surface is parallel to the Ω-loop area (a region from the Gla-domain known to play a role in membrane binding [46, 47]), with the loop penetrating about 4 Å into the phospholipids, both APC models seem reasonable. As seen in Figure 2, APC

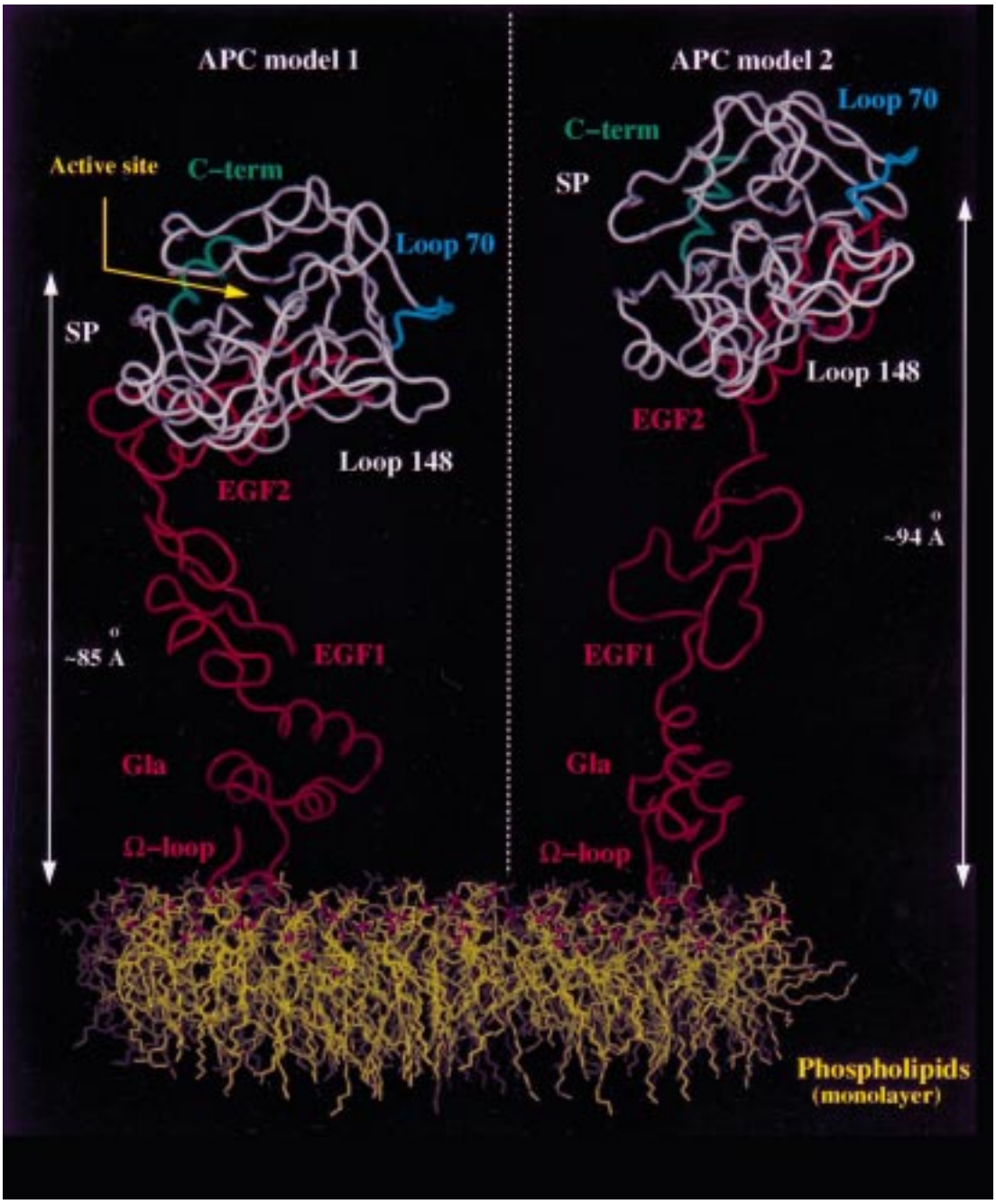

Figure 2. APC-model 1 and model 2. The two models are presented with a view down the active site (model 1, a model for the Gla-domain, holo form, was grafted onto the Gla-domainless APC X-ray structure; model 2, the Gla and EGF1-domains were relocated according to the X-ray structure of FVIIa). The catalytic domain (SP) is in white with the C-term helix coloured in green and the loop 70 (calcium binding loop) coloured in blue for orientation. The light chain (Gla-EGF1-EGF2) is in red. The Gla-domain Ω-loop should be in contact with the cell membrane. A phospholipid monolayer (extracted from Reference 65) is presented in yellow (phosphorus atoms are in magenta) and overall distances between the membrane surface and the active site of APC are shown.

Table 1. Hydrodynamic parameters of human PC and APC in the presence and absence of calcium ions. Stokes radii were determined by size exclusion chromatography. The conformational parameters were calculated as described in 'Materials and methods', using partial specific volumes, determined from the amino acid composition

	PC 2.5 mM $CaCl_2$	APC 2.5 mM $CaCl_2$	PC 5 mM EDTA	APC 5 mM EDTA
v; partial specific volume (cm^3/g)	0.735	0.736	0.735	0.736
Stokes radius (Å)	33.15	34.19	36.43	34.93
Frictional ratio f/f_0	1.263	1.302	1.388	1.33
Axial ratio a/b for $\delta = 0.35\ g_{water}/g_{protein}$	2.94	3.45	4.55	3.77

model 2 is more extended than model 1. However, it is not possible for the time being to define which of the two models represents more accurately APC in solution. The linker region between the EGF1 and EGF2 of APC is most likely flexible, thus allowing the molecule to adopt a range of conformations. Indeed, flexibility between the domains (essentially between the two EGF domains) of FVIIa, either alone in solution or upon binding to tissue factor, has been reported and suggested to play a key role for the catalytic activity of this enzyme toward macromolecular substrates [48]. Similar local conformational re-organisation of the light chain is thus expected for APC/PC, during the interactions with protein S or the thrombin-thrombodulin(-EPCR) complex, while the scaffold of individual APC/PC domains should be relatively rigid.

The overall distance between the active site of APC and the membrane surface could be somewhat longer by choosing another angle between the Gla-domain and the first EGF. Additional biophysical data would be required to further refine our models; however, it is possible to use these structures to probe interactions with, for instance, the A domains of factor Va [49] or factor VIIIa [50].

Full-length protein C models (model 1 and model 2)

Sequence (Figure 1) and structural analysis suggest that it is possible to model PC (the zymogen form) using the X-ray structure of prethrombin 2 or chymotrypsinogen (i.e., PC residues in the activation peptide region can adopt the gross conformation observed in the corresponding segments of these two related proteins). Indeed, such concepts have been used by Fisher et al. [51] and Fuentes-Prior et al. [34] to model PC zymogen. The structure of the linker segment between the EGF2 and the activation segment is easier to predict than the activation peptide as the serine protease domain and the light chain are covalently linked via a disulphide bond (C141 in the light chain with C122, chymotrypsinogen numbering and residue 277 in the PC numbering). Because such an S-S bond is also present in the X-ray templates, this part of the PC model has to adopt a similar conformation as the experimental structures. However, the region running between PC residues 154 to 160 is more difficult to predict, although this part is also present in prethrombin 2. Yet, in all studies on PC modelling, this segment is expected to follow the overall orientation seen in related serine protease zymogens [10, 34, 51]. Our PC model superimposes well onto the structure reported by Fisher et al. [51] at the level of the activation peptide region while some differences are noted at the level of residues 133 to 139. In this previous PC model [51], this segment runs toward the C-terminal helix while it is now known, after solution of the APC structure, that this connecting loop to the EGF2 domain is oriented differently.

In order to assess the overall accuracy of our zymogen model, we used ProStat (Biosym-MSI) to evaluate the stereochemistry and 3D-Profile to search for segments potentially misfolded [52]. The bond lengths and angles of the PC model are clearly acceptable. The 3D-Profile plots (computed for PC and prethrombin 2) indicate that both structures are well folded as the compatibility scores are essentially above 0 [52]. Yet, the scores for the region of PC residues 154 to 160 are low (Figure 3). Interestingly, the equivalent segment

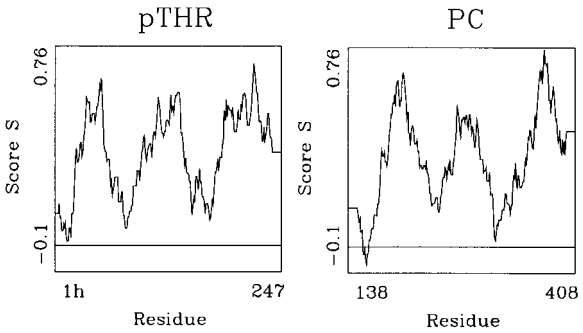

Figure 3. Profile plot for the predicted PC-model and the prethrombin 2 X-ray structure. The compatibility score for residues in a 21-amino acid sliding window is presented. PC refers to protein C and only residues 138 to 408 (PC numbering) are shown, in order to be able to compare with the prothrombin (pTHR) profile (in the PDB file, the first residue is named residue 1h, the numbering here follows the chymotrypsinogen nomenclature, see text). The horizontal line inside the graph represents the 0 value. These profiles indicate that both proteins are correctly folded but the region of the activation peptide has relatively low scores (see text). The other region with low scores in both graphs involves the so-called 148-loop (or autolysis loop). This extended loop is flexible and its structure is not well defined.

in the X-ray structure of prethrombin has also low scores. This observation suggests that the structure in this region of prethrombin is most likely not optimally folded. It is known that the 3D structure of a peptide segment within a macromolecule will generally have to undergo conformational changes in order to be cleaved by enzymes such as serine proteases. Indeed, if the segment to be cleaved were to be rigid and perfectly complementary to the enzyme active site cleft, the protein would be an inhibitor instead of a substrate. Also, we have attempted to plug several PC models into the active site of thrombin using a structure of the activation peptide area modelled in a manner similar to the one used in the present study and noted that such segments did not fit well into the thrombin active site [10]. This suggests that the activation peptide is relatively flexible and could undergo conformational changes upon interaction with the thrombin-TM system. Possibly, Nature generates such activation peptides by creating segments that do not pack optimally against the remaining part of the molecules. Thus, the energetic strains due to the lack of contact or to slightly unfavourable intra-molecular interactions should facilitate local conformational changes and cleavage of the activation peptide. It is thus possible that the relatively poorly folded structure of the activation segment of prethrombin 2 is a common feature to many serine protease zymogens.

The PC zymogen SP domain model was then grafted onto the two light-chain structures developed above to generate two full-length PC zymogen models (Figure 4). Table 1 shows that there are no significant differences in Stokes radius while the axial ratio of the zymogen is somewhat smaller when compared to APC (PC total long axis a = 130 Å and axes b = 40 Å). It is therefore reasonable to model PC as an extended molecule but additional information is needed to fully assess that its long molecular axis is somewhat shorter than the one of the activated enzyme.

In fact, several other experimental data support the modelling of PC zymogen activation peptide in a conformation similar to the ones observed in related zymogen structures and in an extended conformation at the level of the light chain. First, mutagenesis and modelling studies [10, 53] suggest that during the activation process loops 37 and 60 of PC contact TM but not thrombin. Second, by using a distant restraint function added to the forcefield energy expression to force the PC activation peptide a few amino acids before and after the P1 residue (R169 in PC), towards the canonical conformation of a peptide docked into a serine protease active site while interactively docking PC into a preliminary model of the T-TM complex, we noticed that the PC Gla-domain would point toward the membrane surface [10]. However, it has been suggested [11] that the polarity of the main chain (backbone atoms) of the PC activation peptide could run opposite to the one observed in prethrombin 2 and chymotrypsinogen. We have tried to build such a modified activation peptide segment but in this situation, when docking this PC model into a T-TM complex, we observed that the Gla-domain of PC would project in the direction opposite to the membrane surface (about 80–100 Å above the phospholipids), into the solvent. In addition to such a 3D model, PC loops 37 and 60 would be nearby the 60-loop of thrombin but not close to TM and as such would not be consistent with previously reported mutagenesis studies [10, 53]. APC molecule with an inverse polarity of the chain within the activation peptide segment could also result in the formation of a macromolecular complex with the T-TM system but this seems unlikely since experimental data suggest that the Gla-domain of PC interacts with the membrane during the activation process [54, 55]. Furthermore, it has been proposed that the Gla-domain of PC binds to the membrane anchored-EPCR molecule during the activation by the thrombin-TM complex (reviewed in [1]). Molecular modelling study proposes that the maximum height of EPCR above

Table 2. Predicted binding sites for APC and PC. The APC/PC binding sites are presented in Figure 5. PC binding sites are essentially similar to the ones identified for APC but for the APC cluster 2 which is in part covered in PC by the activation peptide segment. Part of this segment, running between the C-terminal part of the EGF2 and the N-terminal residue of the SP domain was depicted as putative binding site. This region involves residues K138, W145, K146, K150, K151, R152, R178, and W234 and could be well located for TM and/or thrombin binding

APC/PC clusters	Main location	Proposed (known) functions (see text for references)
Cluster 1 (top score): Q49, L51, V52, L53, P54, L55, E56, P58, F76, R87, F88	EGF1	Possible role in binding substrates and cofactors
Cluster 2: R143, P144 from the light chain and SP domain L137(296), F203(368), W207(372)	SP-domain	Not known
Cluster 3: light chain D101, L102 and SP domain E129(287), Q131(290), Q134(293), E135(294)) together with residues from cluster 2	EGF2 + SP-domain	Not known
Cluster 4: L51, C59, C63, H66, T68, W84, V93	EGF1 + linker to EGF2	Possible role in binding substrates and/cofactors
Cluster 5: E192(357), Y143(302), F153(316), L73(228), L40(194), K39(193), K37(191)	SP-domain, within the S′ region of the catalytic cleft	Role in FVa, perhaps FVIIIa binding, role in catalytic activity, role in TM and heparin binding, role in serpin interactions
Cluster 6: L13, Gla 14, C17, I18, I21, F40, W41, K43, H44	Gla-domain	Possible interaction with protein S, FVa and FVIIIa, EPCR
Cluster 7: F157(320), K159(322), I184a(348), L185(349), R187(352)	SP-domain of APC and close to the loop 148	Possibly this site plays a role in FVa or FVIIIa binding
Cluster 8: F95, L96, R116, R117, W117, L130, L131	EGF2	Appropriately located for interactions with cofactors or macromolecular substrates.
Cluster 9: F31, D35, D36, A39, F40	Gla-domain	Could contact protein S or EPCR or the C-domains of FV/FVa or FVIII/FVIIIa
Cluster 10: P164(327), P161(324), I184a(348), L185(349), E170(333), E167(330)	SP-domain	Not known
Cluster 11: M59(213), D60(214), K62(217), K63(218), E87(242), V88(245), F89(244), V90(245)	SP-domain	Part of this site seems to bind protein C inhibitor, heparin and TM
Cluster 12: H57(211), C58(212), W215(380), A41(195), C191(356)	SP-domain, active site area	Contact with substrates and serpin inhibitors

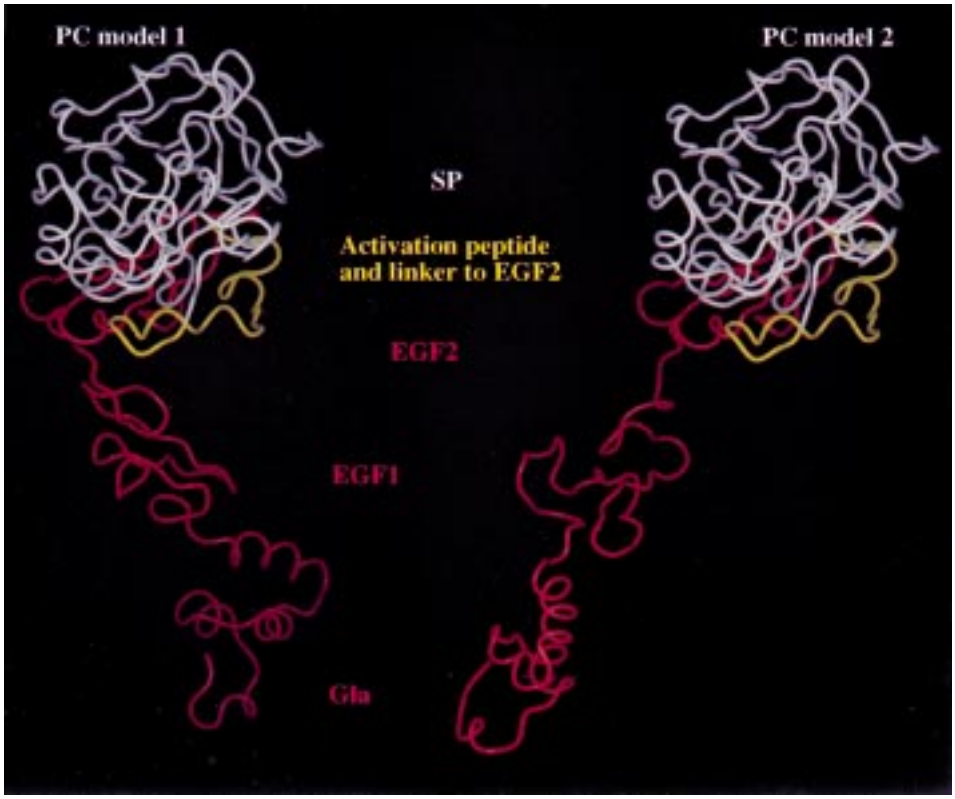

Figure 4a. PC-model 1 and model 2. The PC-models 1 and 2 are shown as ribbons with a view down the active site. The SP-domain is in white, with the segment connecting the light chain with the heavy chain (including the activation peptide) in yellow (the residues involved are from G142 to R169). The light chain is in red.

the membrane plane is about 40–50 Å [56]. Taken together, these observations suggest that during the activation of PC, in order for the activation peptide to properly insert into the thrombin active site cleft and for the Gla-domain to point toward EPCR (or the membrane), the activation segment of PC adopts a 3D structure similar to the one of chymotrypsinogen or prethrombin 2. In fact, preliminary docking of a PC model into the X-ray structure of the TM-thrombin complex reported recently [34] refines but supports the main conclusions resulting from our previous modelling study [10]. Therefore, we consider that our PC models represent approximately the structure of the molecule in solution and can be used to study further the activation process and to search for potential binding sites.

Predicted binding sites: Correlation with biochemical studies

Interfaces of protein-protein recognition sites have been studied in detail [19, 23–25, 27, 57] and the variety of residues, present in these regions, is large. This is in part expected, due to the difference in binding affinity and specificity observed in different biological systems. For instance, two proteins may have to interact transiently for a functional reason, while some others will have to remain tightly associated. The type of molecular surface exposed for binding has also to allow a given amino sequence to adopt a native fold. Thus, even if a larger solvent exposed hydrophobic cluster would be beneficial to a given reaction, such a patch may induce misfolding or aggregation. A cluster of hydrophobic/aromatic residues and/or charged amino acids, exposed at the surface of a molecule, indicates the presence of a potential binding site. However, binding surfaces can be very complex and extended with only little contribution of each amino acid to the total free energy of binding. Hydrophobic interactions between residues at the interface are energetically favourable, but are not very specific, and thus tend to be supplemented by hydrophilic ones (e.g., H-bonds, salt bridges). Furthermore, the hydrophobic effect has been proposed to act differently, depend-

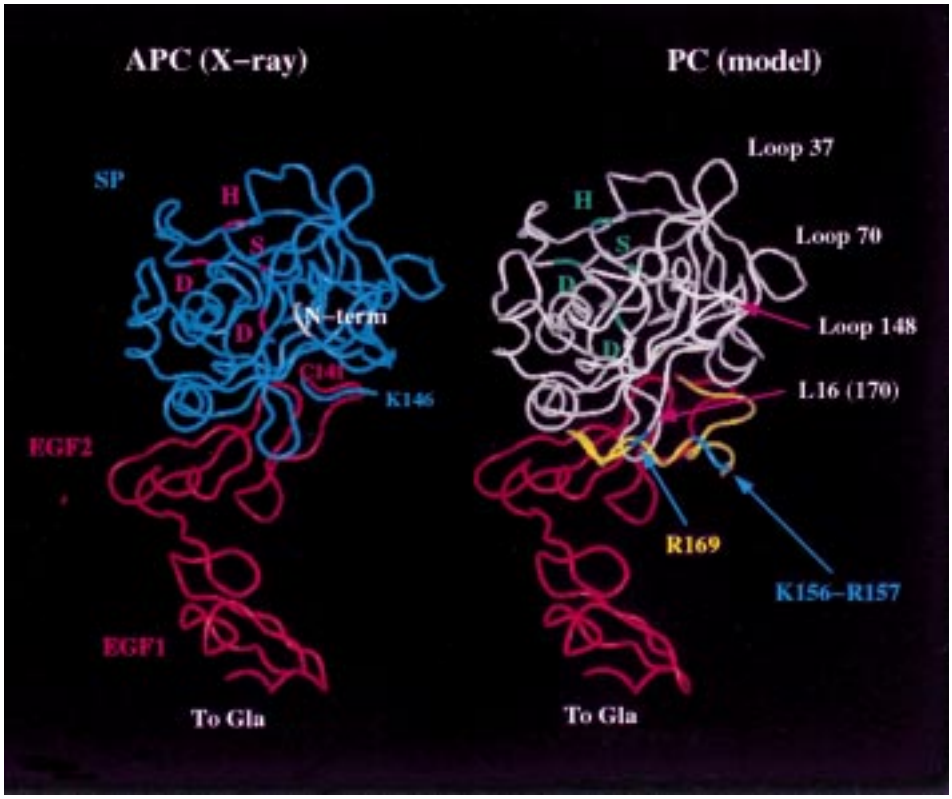

Figure 4b. Overall comparison between APC and PC. Gla-domainless APC X-ray structure and Gla-domainless PC-model (model 1) are shown with a view down the active site. The SP-domain of APC is in blue with the three N-term residues in white (residues 16 to 18 in the chymotrypsinogen numbering corresponding to residues 170 to 172 in the PC numbering). The light chain is in red up to C141 while the next five residues are in blue. The active site triad involves from left to right residues D102, H57 and S195 (magenta). The residue at the bottom of the specificity S1 pocket (below the triad), D189, is also shown for orientation (magenta). Cysteine 141 is disulphide-bonded to C122 from the serine protease domain. Lys 146 is the last residue from the light chain present in the X-ray structure. With regard to the PC-model, the SP-domain is in white with a few loops labelled for orientation. Some key residues, important for the catalytic activity upon activation, are coloured green. The segment running from residues 142 to 168 is in yellow, the P1-residue (R169, i.e., thrombin cleaves the peptide bond between residue 169 and 170) is in dark blue and leucine 16 (which inserts into the SP-domain after activation, corresponding to residue 170 in the PC numbering) is also labelled. The segment K156-R157, often removed by an as yet unknown enzyme, is present here. The activation peptide, when the segment 156-157 is cleaved off, therefore involves residues 158 to 169.

ing on the size of the hydrophobic surface exposed to the solvent [21]. Thus, generalization and definition of recognition sites is not trivial. Despite these limitations and as discussed in previous studies evaluating the role of surface exposed hydrophobic clusters or analysing protein-protein interactions [19, 21, 23–25, 27, 57], hydrophobic patches are often found at molecular interfaces. In fact, theoretical enumeration of binding sites, based upon surface hydrophobicity, has been used successfully to pinpoint key binding regions of several proteins, belonging to different family types [19, 28–30]. It is likely that not all predicted binding surfaces play a role *in vivo*. Also, in some cases, a cluster might be identified and given a top score, while its role has not yet been established experimentally.

Prior to performing calculations on the PC/APC models, we decided to test again theoretical prediction of binding sites on the modified X-ray structure of thrombin. This molecule is a multifunctional serine protease that interacts with many proteins (reviewed in [9]). Interestingly, the top score identified a cluster of residues (M32, F34, R35, K36, Q38, L65, R67, T74, R75, Y76, I82) that are known, due to experimental data, to interact with TM [33–34, 58] or with substrates/inhibitors [9]. Several other sites were consistent with known experimental data, but are not reported here for the sake of clarity. These data suggest again that the approach used in the present article allows for the identification of some key functional regions.

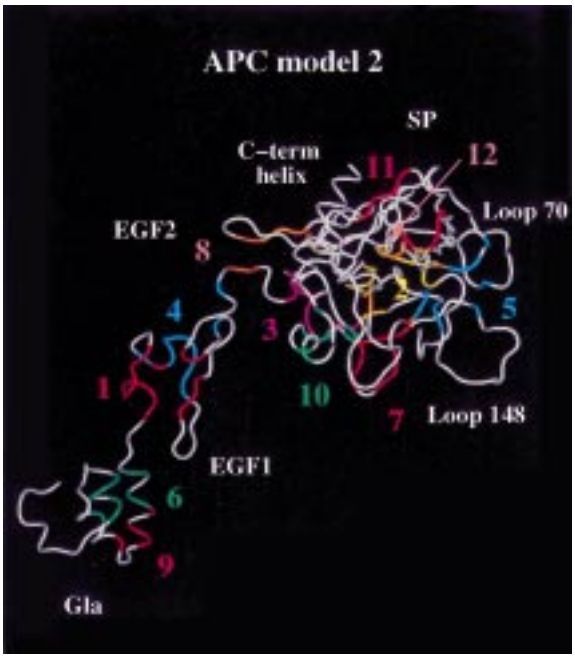

Figure 5. Theoretical enumeration of potential binding sites on APC. Shown are different surface areas, presenting characteristics of a putative binding site as predicted by theoretical means (see also Table 2). Some of these regions are discussed in the text.

Enumeration of binding sites for APC and PC (models 1 and 2) was then carried out. Because evaluations performed on all PC/APC models gave rise to very similar lists of clusters, we decided to combine these data and to discuss only some regions (Table 2, Figure 5). The top score at the surface of APC is found on the first EGF. This region in APC seems to be well positioned for interaction with the EGF1 of protein S or with the discoidin domains of FVa or FVIIIa or with EPCR. Indirect evidence suggests that indeed the EGF1-domain of APC could interact with protein S [59].

Cluster 2 is essentially located at the surface of the serine protease domain. Part of this area is expected to be covered by the activation peptide and may be of functional importance after activation. For the time being, the role of this region is not known. However, since APC and PC make use of the same molecular surface to bind EPCR (i.e., EPCR binds both, PC and APC), the area of cluster 2 should not be involved in EPCR binding, as it is only present in APC.

Cluster 4 is at the surface of EGF1 and linker to the second EGF. As mentioned above for cluster 1, this part of the APC light chain seems well located to play a role during interaction with cofactors and macromolecular substrates. In fact, a peptide running from R81 to F95 (within the light chain) has been suggested as potential binding site for FVa [60].

Cluster 5 is at the surface of the SP-domain, within the S′ region of the catalytic cleft. Several residues included in our list have been experimentally shown to be involved in protein binding. Based on peptide inhibition, residues 149c-154 of hAPC have been suggested to play a role in binding of FVa [61]. Based on loop grafting experiments, we have reported that some residues from loop 148 of APC play an important role in the kinetic properties (kcat and Km) of the enzyme [39] and as such could contact substrates/inhibitors. Molecular modelling and site directed mutagenesis suggest that the loops 37, 60 and 70 of PC are involved in TM interaction [10, 34, 53]. Furthermore, it is known that the loops 37 and 60 are important for heparin binding, protein C inhibitor and α1-antitrypsin interactions [62, 63]. Also, the role of E192 is well established for substrate and serpin interactions as its substitution by a Q results in an APC molecule more efficiently inhibited by α1-antitrypsin, antithrombin or more active in the degradation of FVa [64].

Cluster 6 involves residues from the Gla-domain. This cluster is part of the ‘aromatic stack’ area of the Gla-domain. It is known that the helical stack region from the Gla-domain of factor VIIa interacts with the C-terminal tissue factor domain [13]. After molecular modelling, we also noticed that the Gla-domain of protein S has some surface exposed hydrophobic/aromatic side chains at the level of the Gla-domain helical stack, within the thrombin sensitive region (TSR) and on the first EGF [12]. As it is known that at least the TSR and EGF1-domain of protein S are important for its APC cofactor function, it seems plausible that some amino acids from cluster 6 play a role in protein S binding. Because it has been suggested that the Gla-domain of APC/PC is involved in the binding of EPCR [1], cluster 6 could be important for this purpose.

Cluster 11 is in the SP-domain. We have recently reported that residues K62 and K63 were involved in heparin binding, while these amino acids seem to also play a role in the interaction with the protein C inhibitor [62]. Moreover, these two lysines seem to interact with TM during the activation of PC by the thrombin-TM complex [10, 34].

Conclusions

In the present report we describe model structures of PC/APC. The selected elongated shapes of these 3D-models are in good agreement with the hydrodynamical parameters that we report therein. Screening the molecular surfaces of the constructed models allowed for identification of several binding sites that have already been established experimentally. However, some new areas, that we propose to be located on the surface of the light chain of PC/APC, are compatible with recognition sites for protein S and/or FVa/ FVIIIa and/or EPCR. Further, a region nearby the activation peptide of PC could play a role during the activation by the T-TM-complex. Our data should therefore be valuable to help designing new experiments, aiming at the investigation of physiologically relevant recognition sites at the surface of APC/PC-molecules. The resulting experimental data will in turn be used to refine our structural models.

Acknowledgements

We are grateful to Astra Anderson for providing purified protein C and APC. This project was supported by research grants from La Fondation pour le Recherche Médicale (FRM to B.V.), Malmö University Hospital and from the Swedish National Network for Cardiovascular and Inflammation Research, from the Swedish Medical Research Council (project no. 07143 and 11793), the Louis Jeantet Foundation of Medicine and a Senior Investigators Award from the Swedish Foundation for Strategic Research. Coordinate files for the PC/APC models can be obtained at http://www.klkemi.mas.lu.se/dahlback or via email.

References

1. Esmon, C.T., Gu, J.M., Xu, J., Qu, D., Stearns-Kurosawa, D.J. and Kurosawa, S., Haematologica, 84 (1999) 363.
2. Dahlbäck, B., Semin. Hematol., 34 (1997) 217.
3. Nesheim, M., Wang, W., Boffa, M., Nagashima, M., Morser, J. and Bajzar, L., Thromb. Haemost., 78 (1997) 386.
4. Kalafatis, M., Egan, J.O., van't Veer, C., Cawthern, K.M. and Mann, K.G., Crit. Rev. Eukaryot. Gene Expr., 7 (1997) 241.
5. Shen, L. and Dahlbäck, B., J. Biol. Chem., 269 (1994) 18735.
6. Thorelli, E., Kaufman, R.J. and Dahlbäck, B., Blood, 93 (1999) 2552.
7. Foster, D.C., Sprecher, C.A., Holly, R.D., Gambee, J.E., Walker, K.M. and Kumar, A.A., Biochemistry, 29 (1990) 347.
8. Esmon, C.T., J. Biol. Chem., 264 (1989) 4743.
9. Di Cera, E., Dang, Q.D. and Ayala, Y.M., Cell. Mol. Life Sci., 53 (1997) 701.
10. Knobe, K.E., Bernsdotter, A., Shen, L., Morser, J., Dahlbäck, B. and Villoutreix, B.O., Proteins, 35 (1999) 218.
11. Mather, T., Oganessyan, V., Hof, P., Huber, R., Foundling, S., Esmon, C. and Bode, W., EMBO J., 15 (1996) 6822.
12. Villoutreix, B.O., Teleman, O. and Dahlbäck, B., J. Comput.-Aided Mol. Design, 11 (1997) 293.
13. Banner, D.W., D'Arcy, A., Chene, C., Winkler, F.K., Guha, A., Konigsberg, W.H., Nemerson, Y. and Kirchhofer, D., Nature, 380 (1996) 41.
14. Brandstetter, H., Bauer, M., Huber, R., Lollar, P. and Bode, W., Proc. Natl. Acad. Sci. USA, 92 (1995) 9796.
15. McCallum, C.D., Hapak, R.C., Neuenschwander, P.F., Morrissey, J.H. and Johnson, A.E., J. Biol. Chem., 271 (1996) 28168.
16. Yegneswaran, S., Wood, G.M., Esmon, C.T. and Johnson, A.E., J. Biol. Chem., 272 (1997) 25013.
17. Mutucumarana, V.P., Duffy, E.J., Lollar, P. and Johnson, A.E., J. Biol. Chem., 267 (1992) 17012.
18. Ashton, A.W., Boehm, M.K., Johnson, D.J., Kemball-Cook, G. and Perkins, S.J., Biochemistry, 37 (1998) 8208.
19. Young, L., Jernigan, R.L. and Covell, D.G., Protein Sci., 3 (1994) 717.
20. Jones, S. and Thornton, J.M., Proc. Natl. Acad. Sci. USA, 93 (1996) 13.
21. Lum, K., Chandler, D. and Weeks, J.D., J. Phys. Chem. B, 103 (1999) 4570.
22. Zhang, C., Chen, J. and DeLisi, C., Proteins, 34 (1999) 255.
23. Tsai, C.-J. and Nussinov, R., Protein Sci., 6 (1997) 1426.
24. Tsai, C.-J., Lin, S.L., Wolfson, H.J. and Nussinov, R., Protein Sci., 6 (1997) 53.
25. Jones, S., Marin, A. and Thornton, J.M., Protein Eng., 13 (2000) 77.
26. Janin, J., Proteins, 28 (1997) 153.
27. Dasgupta, S., Iyer, G.H., Bryant, S.H., Lawrence, C.E. and Bell, J.A., Proteins, 28 (1997) 494.
28. Villoutreix, B.O., Härdig, Y., Wallqvist, A., Covell, D.G., García de Frutos, P. and Dahlbäck, B., Proteins, 31 (1998) 391.
29. Blom, A.M., Covell, D.G., Wallqvist, A., Dahlbäck, B. and Villoutreix, B.O., Biochim. Biophys. Acta, 1388 (1998) 181.
30. Caffrey, M., Cai, M., Kaufman, J., Stahl, S.J., Wingfield, P.T., Covell, D.G., Gronenborn, A.M. and Clore, G.M., EMBO J., 17 (1998) 4572.
31. Wang, D., Bode, W. and Huber, R., J. Mol. Biol., 185 (1985) 595.
32. Vijayalakshmi, J., Padmanabhan, K.P., Mann, K.G. and Tulinsky, A., Protein Sci., 3 (1994) 2254.
33. Mathews, II, Padmanabhan, K.P., Tulinksy, A. and Sadler, J.E., Biochemistry, 33 (1994) 13547.
34. Fuentes-Prior, P., Iwanaga, Y., Huber, R., Pagila, R., Rumennik, G., Seto, M., Morser, J., Light, D.R. and Bode, W., Nature, 404 (2000) 518.
35. Soriano-Garcia, M., Padmanabhan, K., de Vos, A.M. and Tulinsky, A., Biochemistry, 31 (1992) 2554.
36. Bernstein, F.C., Koetzle, T.F., Williams, G.J.B., Meyer, E.F. Jr., Brice, M.D., Rodgers, J.R., Kennard, O., Shimanouchi, T. and Tasmui, M., J. Mol. Biol., 112 (1977) 535.
37. Villoutreix, B.O., Åkerström, B. and Lindqvist, A., Blood Coag. Fibrinol., 11 (2000) 261.
38. Ponder, J.W. and Richards, F.M., J. Mol. Biol., 193 (1987) 775.

39. Shen, L., Villoutreix, B.O. and Dahlbäck, B., Thromb. Haemost., 82 (1999) 1078.
40. Blom, A.M., Mörgelin, M., Öyen, M., Jarvet, J. and Fries, E., J. Biol. Chem., 274 (1999) 298.
41. Velten, M., Villoutreix, B.O. and Ladjimi, M.M., Biochemistry, 39 (2000) 307.
42. Siegel, L.M. and Monty, K.J., Biochim. Biophys. Acta, 112, (1966) 346.
43. Deacon, M.P., Davis, S.S., Waite, J.H. and Harding, S.E., Biochemistry, 37 (1998) 14108.
44. Miyazawa, S. and Jernigan, R.L., Macromolecules, 18 (1985) 534.
45. Waxman, E., Laws, W.R., Laue, T.M., Nemerson, Y. and Alexander Ross, J.B., Biochemistry, 32 (1993) 3005.
46. Zhang, L. and Castellino, F.J., J. Biol. Chem., 269 (1994) 3590.
47. Sunnerhagen, M., Forsen, S., Hoffren, A.M., Drakenberg, T., Teleman, O. and Stenflo, J., Nat. Struct. Biol., 2 (1995) 504.
48. Kemball-Cook, G., Johnson, D.J.D., Tuddenham, E.G.D. and Harlos, K., J. Struct. Biol., 127 (1999) 213.
49. Villoutreix, B.O. and Dahlbäck, B., Protein Sci., 7 (1998) 1317.
50. Pemberton, S., Lindley, P., Zaitsev, V., Card, G., Tuddenham, E.G. and Kemball-Cook, G., Blood, 89 (1997) 2413.
51. Fisher, C.L., Greengard, J.S. and Griffin, J.H., Protein Sci., 3 (1994) 588.
52. Lüthy, R., Bowie, J.U. and Eisenberg, D., Nature, 356 (1992) 83.
53. Gerlitz, B. and Grinnell, B.W., J. Biol. Chem., 271 (1996) 22285.
54. Freyssinet, J.M., Gauchy, J. and Cazenave, J.P., Biochem. J., 238 (1986) 151.
55. Horie, S., Ishii, H., Hara, H. and Kazama, M., Biochem. J., 301 (1994) 683.
56. Villoutreix, B.O., Blom, A.M. and Dahlbäck, B., Protein Eng., 12 (1999) 833.
57. Conte, L.L., Chothia, C. and Janin, J., J. Mol. Biol., 285 (1999) 2177.
58. Sadler, J.E., Thromb. Haemost., 78 (1997) 392.
59. Öhlin, A.K., Bjork, I. and Stenflo, J., Biochemistry, 29 (1990) 644.
60. Mesters, R.M., Heeb, M.J. and Griffin, J.H., Biochemistry, 32 (1993) 12656.
61. Mesters, R.M., Heeb, M.J. and Griffin, J.H., Protein Sci., 2 (1993) 1482.
62. Shen, L., Villoutreix, B.O. and Dahlbäck, B., Thromb. Haemost., 82 (1999) 72.
63. Shen, L., Dahlbäck, B. and Villoutreix, B.O., Biochemistry, 39 (2000) 2853.
64. Rezaie, A.R. and Esmon, C.T., J. Biol. Chem., 25 (1993) 19943.
65. Heller, H., Schaefer, M. and Schulten, K., J. Phys. Chem., 97 (1993) 8360.